Acta Crystallographica Section F
Structural Biology and Crystallization Communications
ISSN 1744-3091

Tingting Ran, Yu Wang, Dongqing Xu and Weiwu Wang*

Key Laboratory of Microbiological Engineering of Agricultural Environment, Ministry of Agriculture, College of Life Sciences, Nanjing Agricultural University, Nanjing 210095, People's Republic of China

Correspondence e-mail: wwwang@njau.edu.cn

Received 6 February 2011
Accepted 14 June 2011

Expression, purification, crystallization and preliminary crystallographic analysis of Cg1458: a novel oxaloacetate decarboxylase from *Corynebacterium glutamicum*

Oxaloacetate decarboxylase catalyses the decarboxylation of oxaloacetate to pyruvate and CO_2. Recently, the *Corynebacterium glutamicum* gene product Cg1458 was determined to be a soluble oxaloacetate decarboxylase. To elucidate the mechanism of oxaloacetate decarboxylation by Cg1458, recombinant Cg1458 was purified and crystallized. The best crystal was grown from 0.2 *M* $MgCl_2$, 0.1 *M* Bis-Tris pH 6.0, 25%(*w*/*v*) polyethylene glycol 3350 using the hanging-drop method. The crystals belonged to space group $P4_32_12$, with unit-cell parameters $a = b = 124.1$, $c = 73.6$ Å. The crystals are most likely to contain a dimer in the asymmetric unit, with a V_M value of 2.27 Å^3 Da^{-1}. A full data set was collected at 1.9 Å resolution using synchrotron radiation on beamline BL17U of SSRF, Shanghai, China. Structure-solution attempts by molecular replacement were successful with PDB entries 3qdf or 2dfu as the template.

1. Introduction

Oxaloacetate decarboxylases (EC 4.1.1.3) catalyze the decarboxylation of oxaloacetate to pyruvate and CO_2. This family includes two subfamilies: a biotin-dependent oxaloacetate decarboxylase subfamily and a cytosolic soluble non-biotin-dependent oxaloacetate decarboxylase subfamily. The biotin-dependent oxaloacetate decarboxylase subfamily mainly consists of membrane-bound oxaloacetate decarboxylase sodium pumps, which have been well studied and generally consist of three subunits (or sometimes four; Dimroth, 1982; Woehlke *et al.*, 1992; Dahinden *et al.*, 2004): a soluble biotinylated α subunit, which catalyses the transfer of a carboxyl group from the substrate to the prosthetic group biotin (Dimroth & Thomer, 1983; Schwarz *et al.*, 1988; Wifling & Dimroth, 1989), and two integral membrane subunits: a β subunit which catalyses the decarboxylation of carboxylated biotin and pumps two sodium ions out of the cell membrane (Laussermair *et al.*, 1989; Jockel *et al.*, 1999; Schmid, Vorburger *et al.*, 2002) and a γ subunit which stabilizes the whole complex by interacting with the α subunit *via* its C-terminus and with the β subunit through its N-terminal transmembrane helix (Schmid, Wild *et al.*, 2002; Dahinden *et al.*, 2005). The crystal structure of the transcarboxylase domain of the α subunit has been determined previously (Studer *et al.*, 2007) and belongs to the TIM-barrel family. Cytosolic oxaloacetate decarboxylases have previously been reported to be present in various bacteria (Plaut & Lardy, 1949; Horton & Kornberg, 1964; O'Brien *et al.*, 1977). Some of them have been purified and fully characterized (Benziman *et al.*, 1978; Ng *et al.*, 1982; Labrou & Clonis, 1999). The gene encoding cytosolic oxaloacetate decarboxylase in *Corynebacterium glutamicum*, *cg1458*, has recently been determined (Klaffl & Eikmanns, 2010), but protein-sequence alignment showed that the gene product Cg1458 has no similarity to any known oxaloacetate decarboxylases and belongs to the fumarylacetoacetase (FAA) family. A *BLAST* sequence search against the PDB showed that Cg1458 shares 30–55% identity to some structures (PDB entries 1saw, 1wzo, 2dfu and 3qdf; Manjasetty *et al.*, 2004; H. Mizutani & N. Kunishima, unpublished work; Seattle Structural Genomics Center for Infectious Disease, unpublished work) of members of the FAA family. From the results of sequence alignment, the metal-coordinated residues in the FAA family were found to be conserved in Cg1458. In the FAA family, *Escherichia coli* HpcE is

Table 1
Data-collection and processing statistics.

Values in parentheses are for the highest resolution shell.

Wavelength (Å)	0.9795
Temperature (K)	100
Crystal-to-detector distance (mm)	250
Rotation range per image (°)	1.0
Total rotation range (°)	90
Space group	$P4_32_12$
Unit-cell parameters (Å)	$a = b = 124.06$, $c = 73.61$
Resolution range (Å)	20–1.90 (2.0–1.90)
Observed reflections	322250 (44347)
Unique reflections	45001
Multiplicity	7.2 (7.1)
$R_{\rm merge}$† (%)	11.8 (57.0)
Completeness (%)	98.4 (97.6)
$\langle I/\sigma(I)\rangle$	8.94 (2.63)
Optical resolution‡ (Å)	1.58

† $R_{\rm merge} = \sum_{hkl}\sum_i |I_i(hkl) - \langle I(hkl)\rangle| / \sum_{hkl}\sum_i I_i(hkl)$, where $I_i(hkl)$ and $\langle I(hkl)\rangle$ are the observed intensity of measurement i and the mean intensity of the reflection with indices hkl, respectively. ‡ Vaguine *et al.* (1999).

bifunctional, with decarboxylase and isomerase activities (Tame *et al.*, 2002), and *Homo sapiens* FLJ36880 has also been proposed to have decarboxylase activity according to the crystal structure (Manjasetty *et al.*, 2004), but none of the FAA proteins have been reported to have oxaloacetate decarboxylase activity. To elucidate the mechanism of the oxaloacetate decarboxylase Cg1458, we cloned and expressed the gene for Cg1458 in *E. coli*. The expressed Cg1458 was purified and crystallized.

2. Materials and methods

2.1. Gene cloning, protein expression and purification

To amplify the *cg1458* gene, PCR was carried out with *Pfu* DNA polymerase using the chromosomal DNA of *C. glutamicum* ATCC13032 as template with the primers AGCT**CATATG**CGTTTTGGACGAATTGC and TGCA**CTCGAG**TTAGGCGTCCACAACTGGGTTG corresponding to the 5′ and 3′ ends, respectively. These primers created restriction sites (shown in bold) for the endonucleases *Nde*I and *Xho*I, respectively, at the 5′ and 3′ ends of the PCR product. The amplified PCR product was digested with *Nde*I and *Xho*I and then ligated into the expression vector pET28a digested with the same restriction enzymes to create the expression construct. This step introduced 20 amino acids with six successive histidines at the N-terminus of the target protein (MGSSHHHHHHSSGLVPRGSH). The construct was verified by restriction-enzyme digestion and DNA sequencing. The plasmid containing *cg1458* was then transformed into *E. coli* C43 (DE3) (Miroux & Walker, 1996). The freshly transformed colony was inoculated and grown at 310 K in Luria–Bertani (LB) medium containing kanamycin (30 µg ml^{-1}) overnight. Overnight cultures of the transformant were diluted 1:100 and grown to an optical density of 0.9–1.0 at 600 nm at 310 K. The cells were induced with 0.5 m*M* IPTG and grown for a further 3 h at 303 K. The induced cells were harvested by centrifugation and the pellet was resuspended in binding buffer consisting of 50 m*M* K_2HPO_4/KH_2PO_4 pH 7.6, 300 m*M* NaCl, 10 m*M* imidazole and 1 m*M* PMSF supplemented just before sonication. Sonication was carried out on ice with 200 W output for a total of 30 min with a sequence of 1 s on and 3 s off. The cell lysate was clarified by centrifugation for 30 min at 15 000 rev min^{-1} (Hitachi Rotor R20A2) and the target protein was purified by immobilized metal-affinity chromatography (IMAC) on Ni–NTA Superflow (Qiagen). Briefly, the supernatant was loaded onto a 2 ml bed volume Ni–NTA column previously equilibrated with binding buffer. After washing the column with binding buffer containing 10, 20 and 50 m*M* imidazole (six bed volumes each), the protein was recovered with elution buffers containing 100 and 250 m*M* imidazole The fractions containing 6×His-tagged Cg1458 were combined and concentrated to approximately 1 ml by centrifugation with an Amicon Ultra-15 filter (Millipore). The concentrated protein sample was then loaded onto a Superdex G-200 (Pharmacia Biotech) column pre-equilibrated with 20 m*M* Tris–HCl pH 8.0 containing 300 m*M* NaCl and the column was eluted with 1.2 bed volumes of the same buffer. The elution pattern showed that there were two protein peaks; these were analyzed by SDS–PAGE and their purity was checked by staining the gels with Coomassie Brilliant Blue R250. Since the first peak appeared at the position of the void volume of the column, we pooled the fractions from the second peak together.

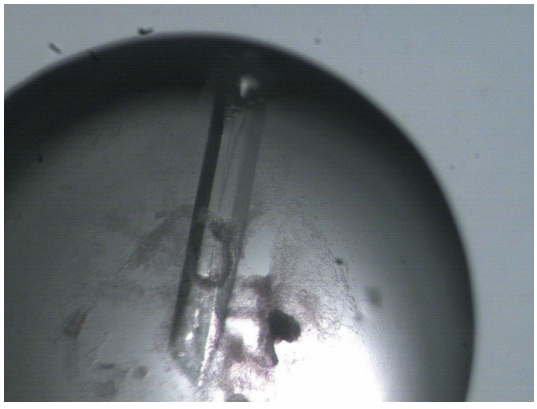

Figure 1
A crystal of Cg1458. Its dimensions were approximately 300 × 40 × 40 µm.

2.2. Crystallization

The protein was concentrated to 20 mg ml^{-1} in 300 m*M* NaCl and 20 m*M* Tris pH 8.0 using an Amicon Ultra-15 filter (Millipore). The concentration was determined from the absorbance at 280 nm, assuming an ε_{280} of 0.8 for a 1.0 mg ml^{-1} protein solution. Initial crystallization screens were performed using six different screening kits from Hampton Research (Index, MembFac, Crystal Screen, Crystal Screen 2, Crystal Screen Lite and Crystal Screen Cryo) employing the sitting-drop vapour-diffusion method. All trials were stored at 295 K. The initial screen yielded rod-shaped crystals from the following condition: 0.2 *M* $MgCl_2$, 0.1 *M* Bis-Tris pH 6.5, 25%(*w*/*v*) polyethylene glycol 3350. The condition was optimized by grid screening of the PEG 3350 concentration and the pH of the crystallization condition. Crystals suitable for diffraction were grown by mixing 1 µl 20 mg ml^{-1} protein solution with the same amount of reservoir solution and equilibrating the drop against 200 µl reservoir solution [0.2 *M* $MgCl_2$, 0.1 *M* Bis-Tris pH 6.0, 25%(*w*/*v*) polyethylene glycol 3350] using the hanging-drop method in 24-well plates. The crystals reached maximum dimensions after 2 d.

2.3. Data collection

Prior to cryocooling, crystals were looped out from the crystallization drop and sequentially transferred into fresh mother liquor, mother liquor with 5% glycerol, mother liquor with 10% glycerol and mother liquor with 15% glycerol for a few seconds each. After transfer to the final solution, the crystal was flash-cooled in liquid nitrogen. Complete X-ray diffraction data sets were collected on beamline BL17U of SSRF, Shanghai, People's Republic of China

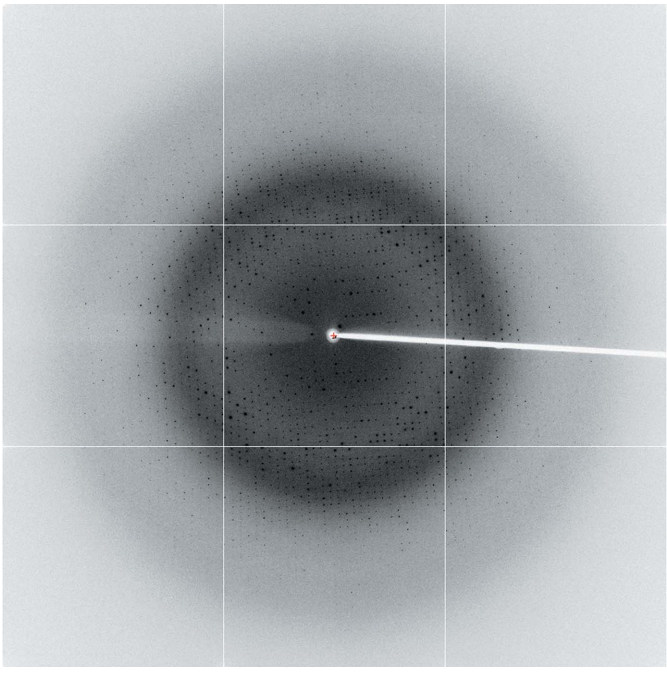

Figure 2
A diffraction image of a Cg1458 crystal.

using an ADSC Q315R detector. The best crystal diffracted to 1.9 Å resolution. Each frame was exposed for 1.2 s with a rotation range of 1.0°. The data were processed using the *XDS* package (Kabsch, 2010*a*,*b*). The data-collection and processing statistics are summarized in Table 1.

3. Results and discussion

Recombinant Cg1458 with a His tag was overexpressed in *E. coli* in a soluble form with a yield of about 15 mg purified protein per litre of culture. Rod-shaped crystals appeared in hanging drops using a reservoir solution consisting of 0.2 *M* $MgCl_2$, 0.1 *M* Bis-Tris pH 6.5, 25%(*w*/*v*) polyethylene glycol 3350 at 295 K in 2 d. Based on this observation, a systematic screening for optimized crystallization conditions was performed. Finally, single crystals with variable size (200–500 × 10–40 × 10–40 µm) were obtained using 0.2 *M* $MgCl_2$, 0.1 *M* Bis-Tris pH 6.0, 25%(*w*/*v*) polyethylene glycol 3350 as precipitant at 295 K in 2 d (Fig. 1). The best diffraction data were collected to 1.9 Å resolution using synchrotron X-rays. The crystals belonged to space group $P4_32_12$, with unit-cell parameters $a = b = 124.1$, $c = 73.6$ Å (Fig. 2). A previous study showed that the protein exists as a dimer (Klaffl & Eikmanns, 2010). Assuming the presence of a dimer in the asymmetric unit, the calculated Matthews coefficient V_M (Matthews, 1968) was 2.27 $Å^3$ Da^{-1}, which corresponds to a solvent content of 45.9%.

Crystal structure determination of Cg1458 by molecular replacement using the crystal structures of 2-hydroxyhepta-2,4-diene-1,7-dioate isomerase from *Thermus thermophilus* HB8 (40% sequence identity between the C-terminal 219 amino acids of Cg1458 and TTHA0809; PDB entry 2dfu; H. Mizutani & N. Kunishima, unpublished work) or *Mycobacterium marinus* (55% sequence identity; PDB entry 3qdf; Seattle Structural Genomics Center for Infectious Disease, unpublished work) as search models was successful. The detailed structure and the decarboxylation mechanism of this protein will be published elsewhere.

This work was supported by the Joint Research Fund of NSFC and CAS for Large-Scale Scientific Facilities (10979028) and the National Fund for Talent Training in Basic Science (J0730647). We thank the staff at beamline BL17U of SSRF, Shanghai, People's Republic of China for their assistance during data collection.

References

Benziman, M., Russo, A., Hochman, S. & Weinhouse, H. (1978). *J. Bacteriol.* **134**, 1–9.
Dahinden, P., Pos, K. M. & Dimroth, P. (2005). *FEBS J.* **272**, 846–855.
Dahinden, P., Pos, K. M., Taralczak, M. & Dimroth, P. (2004). *Arch. Microbiol.* **182**, 414–420.
Dimroth, P. (1982). *FEBS Lett.* **141**, 59–62.
Dimroth, P. & Thomer, A. (1983). *Eur. J. Biochem.* **137**, 107–112.
Horton, A. A. & Kornberg, H. L. (1964). *Biochim. Biophys. Acta*, **89**, 381–383.
Jockel, P., Di Berardino, M. & Dimroth, P. (1999). *Biochemistry*, **38**, 13461–13472.
Kabsch, W. (2010*a*). *Acta Cryst.* D**66**, 125–132.
Kabsch, W. (2010*b*). *Acta Cryst.* D**66**, 133–144.
Klaffl, S. & Eikmanns, B. J. (2010). *J. Bacteriol.* **192**, 2604–2612.
Labrou, N. E. & Clonis, Y. D. (1999). *Arch. Biochem. Biophys.* **365**, 17–24.
Laussermair, E., Schwarz, E., Oesterhelt, D., Reinke, H., Beyreuther, K. & Dimroth, P. (1989). *J. Biol. Chem.* **264**, 14710–14715.
Manjasetty, B. A., Niesen, F. H., Delbrück, H., Götz, F., Sievert, V., Büssow, K., Behlke, J. & Heinemann, U. (2004). *Biol. Chem.* **385**, 935–942.
Matthews, B. W. (1968). *J. Mol. Biol.* **33**, 491–497.
Miroux, B. & Walker, J. E. (1996). *J. Mol. Biol.* **260**, 289–298.
Ng, S. K., Wong, M. & Hamilton, I. R. (1982). *J. Bacteriol.* **150**, 1252–1258.
O'Brien, R., Chuang, D. T., Taylor, B. L. & Utter, M. F. (1977). *J. Biol. Chem.* **252**, 1257–1263.
Plaut, G. W. & Lardy, H. A. (1949). *J. Biol. Chem.* **180**, 13–27.
Schmid, M., Vorburger, T., Pos, K. M. & Dimroth, P. (2002). *Eur. J. Biochem.* **269**, 2997–3004.
Schmid, M., Wild, M. R., Dahinden, P. & Dimroth, P. (2002). *Biochemistry*, **41**, 1285–1292.
Schwarz, E., Oesterhelt, D., Reinke, H., Beyreuther, K. & Dimroth, P. (1988). *J. Biol. Chem.* **263**, 9640–9645.
Studer, R., Dahinden, P., Wang, W.-W., Auchli, Y., Li, X.-D. & Dimroth, P. (2007). *J. Mol. Biol.* **367**, 547–557.
Tame, J. R., Namba, K., Dodson, E. J. & Roper, D. I. (2002). *Biochemistry*, **41**, 2982–2989.
Vaguine, A. A., Richelle, J. & Wodak, S. J. (1999). *Acta Cryst.* D**55**, 191–205.
Wifling, K. & Dimroth, P. (1989). *Arch. Microbiol.* **152**, 584–588.
Woehlke, G., Wifling, K. & Dimroth, P. (1992). *J. Biol. Chem.* **267**, 22798–22803.